Biochemical and Biophysical Research Communications 442 (2013) 234–241

Contents lists available at ScienceDirect

Biochemical and Biophysical Research Communications

journal homepage: www.elsevier.com/locate/ybbrc

Regulation of adult hematopoiesis by the a disintegrin and metalloproteinase 10 (ADAM10)

Silvio Weber [a,1], Sebastian Wetzel [a], Johannes Prox [a], Tobias Lehmann [a], Janna Schneppenheim [a], Marjo Donners [b], Paul Saftig [a,*]

[a] Institut für Biochemie, Christian-Albrechts-Universität zu Kiel, Olshausenstrasse 40, D-24098 Kiel, Germany
[b] Department of Molecular Genetics, Cardiovascular Research Institute Maastricht, Maastricht University, Universiteitssingel 50, 6200 MD Maastricht, The Netherlands

ARTICLE INFO

Article history:
Received 31 October 2013
Available online 15 November 2013

Keywords:
Granulopoesis
Myeloproliferative disorder
Ectodomain shedding
ADAM proteases

ABSTRACT

Adult hematopoiesis requires tightly regulated cell–cell interactions between hematopoietic cells and the bone marrow stromal microenvironment. We addressed the question if the ectodomain sheddase ADAM10 is essential to regulate adult hematopoiesis. Induced ADAM10 deletion in hematopoietic cells resulted in morphological and histological abnormalities that resemble an unclassified myeloproliferative disorder (MPD). The MPD was characterized by an expansion of granulocytic subpopulations and their infiltration of peripheral hematopoietic tissues, the development of hepatosplenomegaly with extramedullary erythropoiesis, lymphnodepathy and death of the mice around 20 weeks after induction. ADAM10 expression analysis during the different stages of the MPD revealed that non-targeted hematopoietic cells repopulated the immune system of the ADAM10-deficient mice. Examination of mice with a myeloid- or epidermis-specific deletion of ADAM10 and bone marrow transplantation (BMT) experiments indicated that the development of the MPD can be triggered by non-cell autonomous effects. We found that plasma levels of clinical markers for MPD such as G-CSF, TIMP-1 and IL-16 were significantly elevated in ADAM10-deficient mice. Our findings indicate that a tightly controlled ADAM10 expression is needed to balance hematopoietic cell-fate decisions in adult mice.

1. Introduction

In recent studies emerging evidence for the crucial role of tightly controlled cell–cell communication between the bone marrow microenvironment and hematopoietic cells during hematopoiesis has been established. However the detailed molecular mechanisms regulating this process have remained elusive so far. A rapid and irreversible posttranslational modification of cell surface protein density can be achieved by an extracellular proteolytic cleavage step which is referred to as "ectodomain shedding" [1–4]. ADAM10 is an ubiquitously expressed protein which is capable of cleaving numerous transmembrane proteins such as Notch receptors [5] that are implicated for proper regulation of hematopoietic development and homeostasis. In order to study the consequence of ADAM10 downregulation during adult hematopoiesis, we conditionally inactivated its expression using the inducible Mx-Cre strain [6] and a myeloid-specific deleter strain [7], respectively. The Mx promoter becomes activated by interferon response or synthetic double-stranded RNA in most cells of immunologically important tissues including bone marrow stroma cells [6]. A similarly induced knockout of the Notch1 receptor and the putative sole downstream signaling mediator *Rbp-j*, led to *de novo* ectopic B-cell development in the thymus from common lymphoid progenitors [8] thus underlining the importance of Notch receptor signaling for cell-fate decisions during lymphopoiesis.

In this study, similar to a recently published report [9], we show that the induced loss of ADAM10 leads to the development and progression of a MPD with concomitant loss of mature B- and T-lymphocytes in the bone marrow, spleen and peripheral blood. The expanded myeloid population mainly consists of $CD11b^+$/$Gr1^+$ cells with normal ADAM10 expression levels. Additionally bone marrow transplantation (BMT) experiments strongly support a non-cell autonomous origin of the MPD which is possibly triggered and maintained by the excessive secretion of G-CSF, TIMP-1 and IL-16.

2. Materials and methods

2.1. Generation of inducible conditional ADAM10 (cKO) mice

The *ADAM10*$^{flox/flox}$ mice were crossed with *Mx*-Cre mice [10], K5-tTA-Cre mice [11] or LysM-Cre mice [7]. To induce

* Corresponding author. Fax: +49 431 8802238.
E-mail address: psaftig@biochem.uni-kiel.de (P. Saftig).
[1] Present address: Heart Research Centre Göttingen, Universitätsmedizin Göttingen, Department of Cardiology and Pneumology, University Göttingen, Göttingen, Germany.

0006-291X/$ - see front matter © 2013 Elsevier Inc. All rights reserved.
http://dx.doi.org/10.1016/j.bbrc.2013.11.020

Mx-mediated deletion of *ADAM10* during adult hematopoiesis, 6-week old *ADAM10*$^{flox/flox}$/Mx-Cre$^{+/-}$ (*ADAM10*$^{-/-}$) and *ADAM10*-$^{flox/flox}$ (Ctr) mice were injected three times in two-day intervals with 250 μg polyinosinic–polycytidylic acid (pI–pC).

2.2. Western blot of tissue lysates

Tissues were uniformly lysed (150 mM NaCl, 2 mM EDTA, 0.8 mM EGTA, 10 mM Tris–HCl, pH 7.4 and Complete Protease Inhibitors (1:25, Roche)). ADAM10 was detected using a polyclonal antiserum (B42.1) (kind gift of W. Annaert, University Leuven), EEF-2 was detected by the Abcam antibody 40812 and actin by a polyclonal antibody from Sigma–Aldrich. The HRP-labeled secondary antibodies were from Dianova, Hamburg, Germany, and detection of chemiluminescence was performed with Amersham ECL Advance Western Blotting Detection Reagent (GE Healthcare, Uppsala, Sweden).

2.3. Histology and immunohistochemistry

Bones, spleen, lymph nodes, liver and skin were fixed by immersion in 4% buffered formalin. For decalcification bones were incubated for 24 h incubation in 1% acetic acid. After overnight postfixation, dehydratation and paraffin embedding 5-μm-sections were either stained with Hematoxylin and Eosin (H&E), Giemsa or processed for immunohistochemistry to show B220 (Immunotools) or Ki-67 (Abcam).

2.4. Magnetic cell separation

HSCs and progenitor cells from bone marrow aspirates were enriched by a negative depletion using the Miltenyi Biotech Lineage Negative Depletion kit according to the manufacture's instructions.

2.5. Flow cytometry

Single-cell suspensions of bone marrow, spleen, lymph nodes were prepared and 5×10^5 cells were stained with the respective antibodies for 45 min at 4 °C. Monoclonal antibodies were FITC-conjugated (CD3e, Gr-1, CD23, CD71), PE-conjugated (CD4, CD11b, CD21, Ter-119) and APC-conjugated (CD8a, F4/80, B220) or unconjugated (ADAM10, BD Biosciences; detection with secondary antibody anti-rat IgG2a, Jackson ImmunoResearch).

2.6. Preparation of bone marrow derived macrophages (BMDM)

Total bone marrow cells were flushed from long bones (tibiae and femur), passed through a nylon sieve (BD Biosciences) and cultured with macrophage growth medium (50% DMEM, 50% PAA Macrophage Growth Medium, 20% FCS, 50 μg/ml Pen/Strep and 20 ng/ml M-CSF (Immunotools, Friesoythe, Germany). For analysis 7-day old BMDMs were harvested using accutase (PAA) and stained for F4/80 (BD Biosciences) to show maturation and enrichment of mature macrophages.

2.7. Serology

Plasma granulocyte-colony stimulating factor (G-CSF), tissue-inhibitor of Metalloprotease 1 (TIMP-1) and thymic stromal lymphopoietin (TSLP) levels were measured according to the instructions in the corresponding DuoSet mouse ELISA kits (R&D Systems).

2.8. Myeloperoxidase (MPO) activity measurement

Myeloperoxidase (MPO) activity was measured in cell suspension of bone marrow, spleen, liver, lymph nodes and skin. After freezing in liquid nitrogen, equal amounts of tissue samples were homogenized and incubated at 60 °C for 2 h and centrifuged for 5 min at 10,000*g*. 10 μl of the supernatant was mixed with 50 μl peroxidase substrate (BM blue POD, Roche). After 10–20 min the reaction was stopped by adding 50 μl 2 M H_2SO_4 and absorbance was recorded at 450 nm.

2.9. Bone marrow transplantations

Six week old *ADAM10*$^{flox/flox}$/Mx-Cre$^{+/-}$ (*ADAM10*$^{-/-}$) and *ADAM10*$^{flox/flox}$ (Ctr) mice were injected three times in two-day intervals with 250 μg polyinosinic–polycytidylic acid (pI–pC) to induce ADAM10 deletion. Two weeks after the last injection recipient mice (3 females and 2 males per group) were lethally irradiated with 6 Gy the day before and the day of transplantation. Control mice were transplanted with 10×10^6 bone marrow cells from littermate ADAM10$^{-/-}$ mice (1 male, 1 female), and vice versa for transplantation of ADAM10$^{-/-}$ bone marrow into control mice. After 6 weeks recovery, mice were used for the analyses.

2.10. Statistical analysis

Statistical significance was performed as unpaired Student's *T*-test using Microsoft Excel software. Error bars indicate the mean ± standard deviation of the mean. *P* values: $^{*}P < 0.05$, $^{**}P < 0.005$, $^{***}P < 0.0005$.

3. Results

3.1. Lack of ADAM10 expression and activity in the adult hematopoietic system

We induced the deletion of the protease in *ADAM10*$^{flox/flox;\ Mx1Cre}$ mice and sacrificed mice 2 weeks after the last injection of double stranded RNA (pI–pC). Genomic deletion was observed in bone marrow, spleen, liver and skin (Fig. 1A). Immunoblot analysis revealed a strong downregulation of ADAM10 protein expression in bone marrow and spleen as well as of the proform of the protease in liver (Fig. 1B). Despite significantly downregulated ADAM10 protein expression (Fig. 1CI) in bone marrow derived macrophages (BMDMs), we could not observe overt alterations in cell morphology (Fig. 1CII) or differentiation status (Fig. 1CIII). Isolated B-lymphocytes from spleens of wild type and induced ADAM10 knock-out mice revealed the downregulation of ADAM10 protein expression and concomitantly diminished CD23 and Notch2 receptor processing (data not shown). Lineage depletion of bone marrow cells to obtain hematopoietic stem (HSC) and progenitor cells was performed. A clear absence of ADAM10 expression in a subset of HSCs (Fig. 1DIII) was demonstrated.

3.2. Phenotypical analysis of pI–pC induced *ADAM10*$^{-/-}$ mice

About 6–12 weeks following the last injection ADAM10-depleted mice start to show fatigue, an apathic behavior and loss of hair especially in facial regions (Fig. 2A). 12 weeks after induction the mice became moribund showing an enlarged liver with thrombocytosis (Fig. 2AI, I'), splenomegaly (Fig. 2AII), lymphnodepathy (Fig. 2AIII) and severe thymic atrophy (Fig. 2AIV). Histological examination revealed an increase of white blood cells in the cavity of long bones (Fig. 2BI, I'), extramedullary hematopoiesis

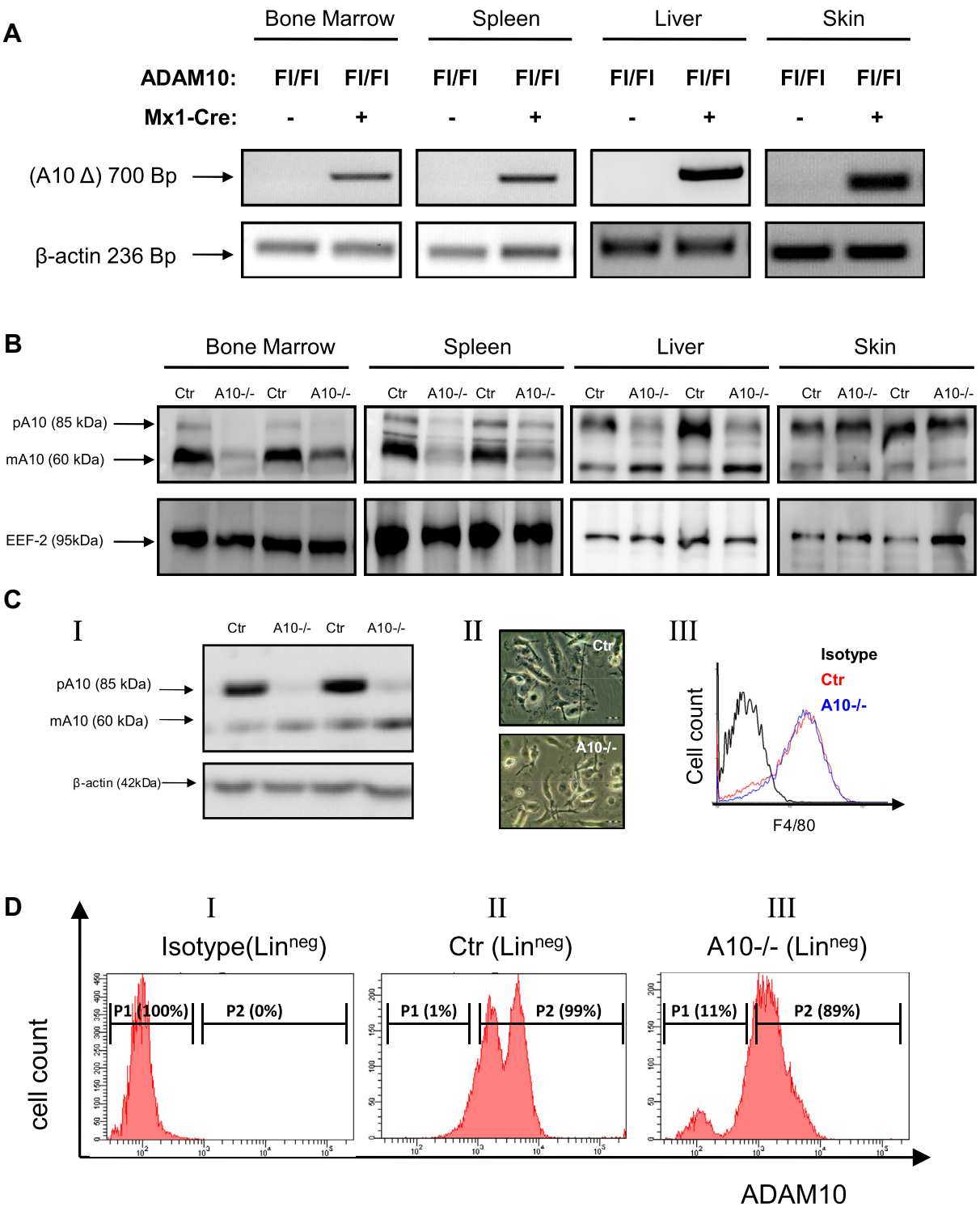

Fig. 1. pI–pC induced deletion of *ADAM10* during postnatal hematopoiesis. (A) PCR analysis on genomic DNA from bone marrow, spleen, liver and skin. Beta actin was used as a house keeping gene control. (B) Western blot analysis of cell homogenates from bone marrow, spleen, liver and skin. pA10: precursor of ADAM10; mA10: mature form of ADAM10. EEF-2: Eukaryotic Elongation Factor-2 was used a loading control. (C) Macrophages developed from bone marrow aspirates (cultured 2 weeks after induction) shows a significant drop in ADAM10 expression (I), undisturbed morphology (II) and differentiation (III). (D) Flow cytometry analysis of lineage depleted bone marrow cells showing targeting efficacy of 11% in hematopoietic stem or progenitor cells in pI–pC induced ADAM10$^{-/-}$ mice 2 weeks after induction.

including infiltration of megakaryocytes in spleen (Fig. 2BII, II'), thrombocytosis in liver (Fig. 2BIII, III') as well as epidermal thickening, cyst formation, hyperproliferation of basal keratinocytes and hyperkeratinization in skin (Fig. 2BIV, IV'). In addition granulocytic infiltration of all histologically examined tissues was observed using the myeloperoxidase (MPO) activity assay (Fig. 2BI''–IV'').

3.3. Dysregulation of hematopoietic balance in primary and secondary hematopoeitic tissues of ADAM10$^{-/-}$ mice

Measurements of total cell counts revealed an initial drop in cellularity 2 weeks after the last injection but this effect diminished during later stages of the analysis (Fig. 3AI). The distribution of cell counts between the different lymphocytic and granulocytic

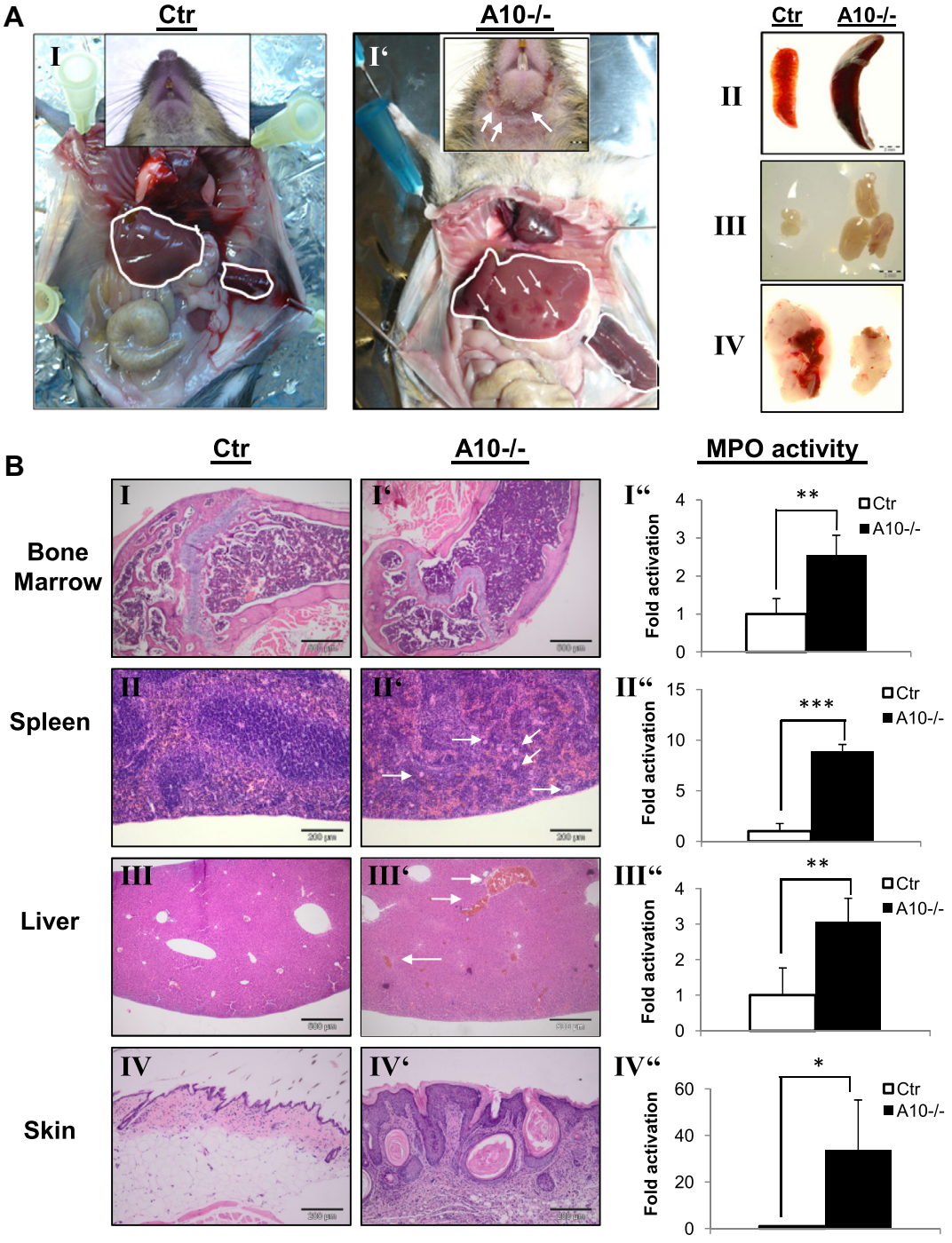

Fig. 2. Morphological and histological examination of *ADAM10*-deleted mice 12 weeks after induction. (A) Morphological analysis of control (Ctr) and ADAM10-deleted cKO mice ($A10^{-/-}$) show hepatosplenomegaly with thrombocytosis and eczema formation in facial regions (I) splenomegaly (II), enlarged lymph nodes (III) and thymic atrophy (IV) in $ADAM10^{-/-}$ mice. Scale bars = 2 mm. (B) Histological analysis revealed an increase in white blood cells in bone marrow of ADAM10-deficient mice. Sections of 20-week-old mice were stained with H&E (I, I'; II, II'; III, III'; IV, IV'). In spleen sections (II, II') of ADAM10 deleted mice an increased occurrence of megakaryocytes (indicated by white arrows) was observed 12 weeks after induction; H&E stained liver sections (III, III') revealed thrombocytosis and granulocyte infiltration. In skin sections (IV, IV') cyst formation, thickened epidermis, hyperproliferation of basal cells and hyperkeratinisation were observed. Scale bars are 500 μm for I, I' and III, III'; 200 μm for II and II', IV, IV'; Myeloperoxidase (MPO) activity assays demonstrate an increase of activity in ADAM10-deficient tissues (I'': bone marrow; II'': spleen; III'': liver; IV'': skin) 12 weeks after induction and potential degranulation activity of mature granulocytes, $n > 3$ for each genotype. Error bars represent SEM. *P*-values: $^{*}P < 0.05$, $^{**}P < 0.005$, $^{***}P < 0.0005$.

populations was significantly altered between wild type and knock-out mice six and twelve weeks after the last pI–pC induction (Fig. 3 AII–IV). The increase in the granulocytic population was mainly due to an increase in $CD11b^{+}/Gr1^{+}$ positive cells. Freshly isolated splenocytes were applied to flow cytometric analysis and revealed a shift in the hematopoietic distribution between lymphocytes and granulocytes. While granulocyte and macrophage cell counts became progressively increased, numbers of mature B- and T-lymphocytes dropped significantly over time (Fig. 3BII–IV).

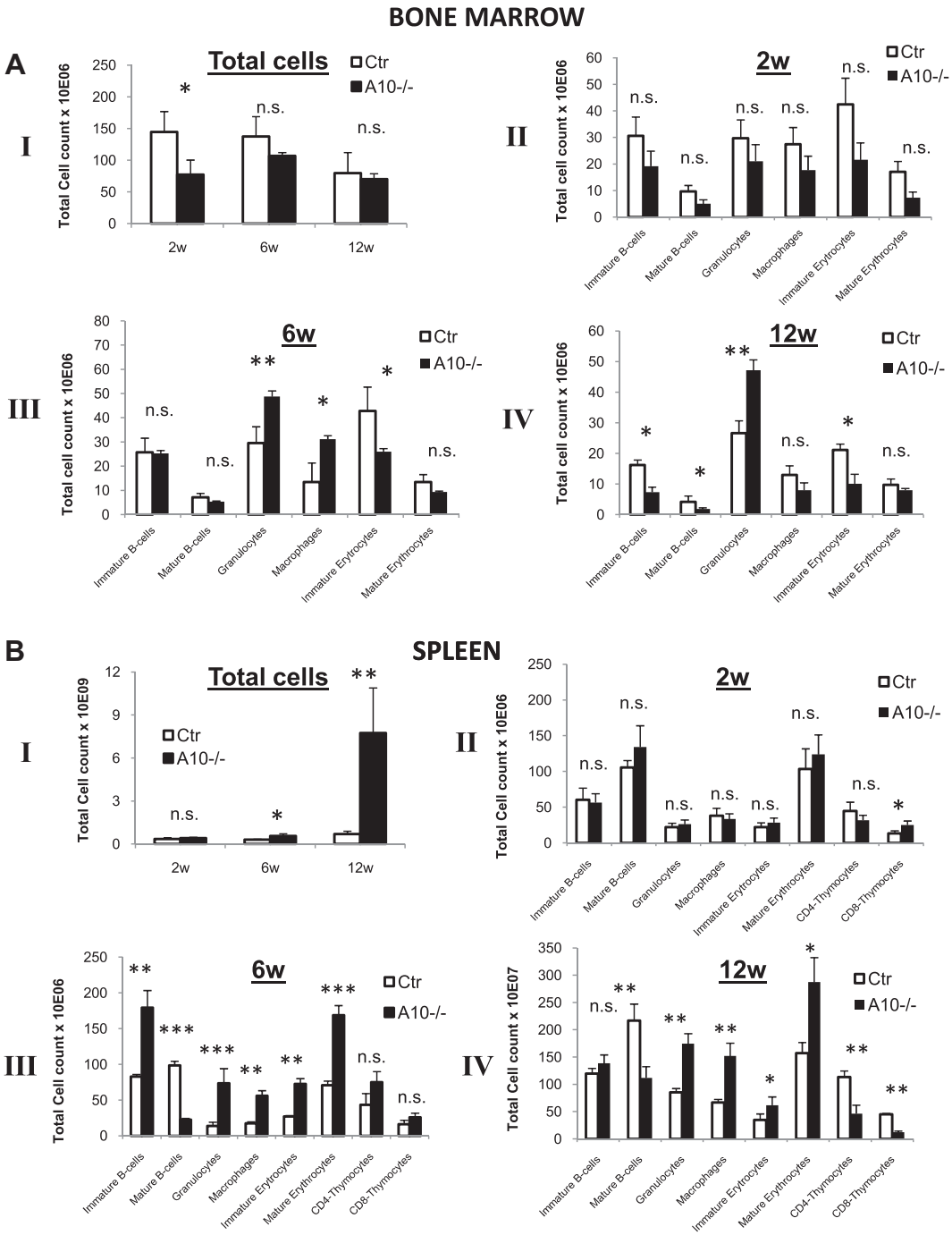

Fig. 3. Development of a defective hematopoietic balance in the bone marrow and spleen of *ADAM10*$^{-/-}$ mice. (A) Analysis of total cell count and selected lymphocyte populations in bone marrow after 2 (II), 6 (III) and 12 (IV) weeks after induction. (B) Analysis of total cell count and selected lymphocyte populations in spleen after 2 (II), 6 (III) and 12 (IV) weeks after induction. Error bars represent SEM. *P*-values: $^{*}P < 0.05$, $^{**}P < 0.005$, $^{***}P < 0.0005$.

3.4. Splenomegaly and extramedullary hematopoiesis in ADAM10-deficient mice

Total cell counts in spleen increased gradually after pI–pC injection with a dramatic rise between six and twelve weeks after pI–pC injection (Fig. 3BI). While granulocytes and macrophages cell counts became progressively increased, numbers of mature B- and T-lymphocytes dropped significantly over time (Fig. 3BII–IV). Other than observed in bone marrow total cell counts of immature B-lymphocytes and erythrocytes were significantly upregulated. The histological examination of the spleen showed enlarged areas of red pulpa and decreased numbers of B-cell follicles (Fig. 2 BII and II'). Extramedullary hematopoiesis seems to be the major cause for the observed irregular distribution of hematopoietic cells in the spleens of induced ADAM10 knock-out mice.

3.5. Development of a myeloproliferative disorder in ADAM10-deficient mice

We analyzed additional tissues such as skin, liver, thymus and lymph nodes. Importantly, in all cases a myeloid infiltration was detectable (data not shown). However, clear morphological changes such as acanthosis, hyperkeratosis and dermal hyperplasia (Fig. 2BIV and IV') were only obvious in the skin. The thymus also

showed a significant block in differentiation from double-negative to double-positive stage T-lymphocytes and an increase in B220 positive B-lymphocytes (data not shown). Wright-Giemsa staining of blood smears showed the development of granulocytosis, thrombocytosis and Pseudo-Pelger Huet formation in ADAM10-deleted mice (data not shown).

3.6. Disruption of ADAM10 in myeloid cells does not lead to a myeloproliferative disorder

To allow discrimination between cell autonomous and non-cell autonomous reasons for the observed myeloid infiltration we decided to conditionally delete ADAM10 also in myeloid cells using

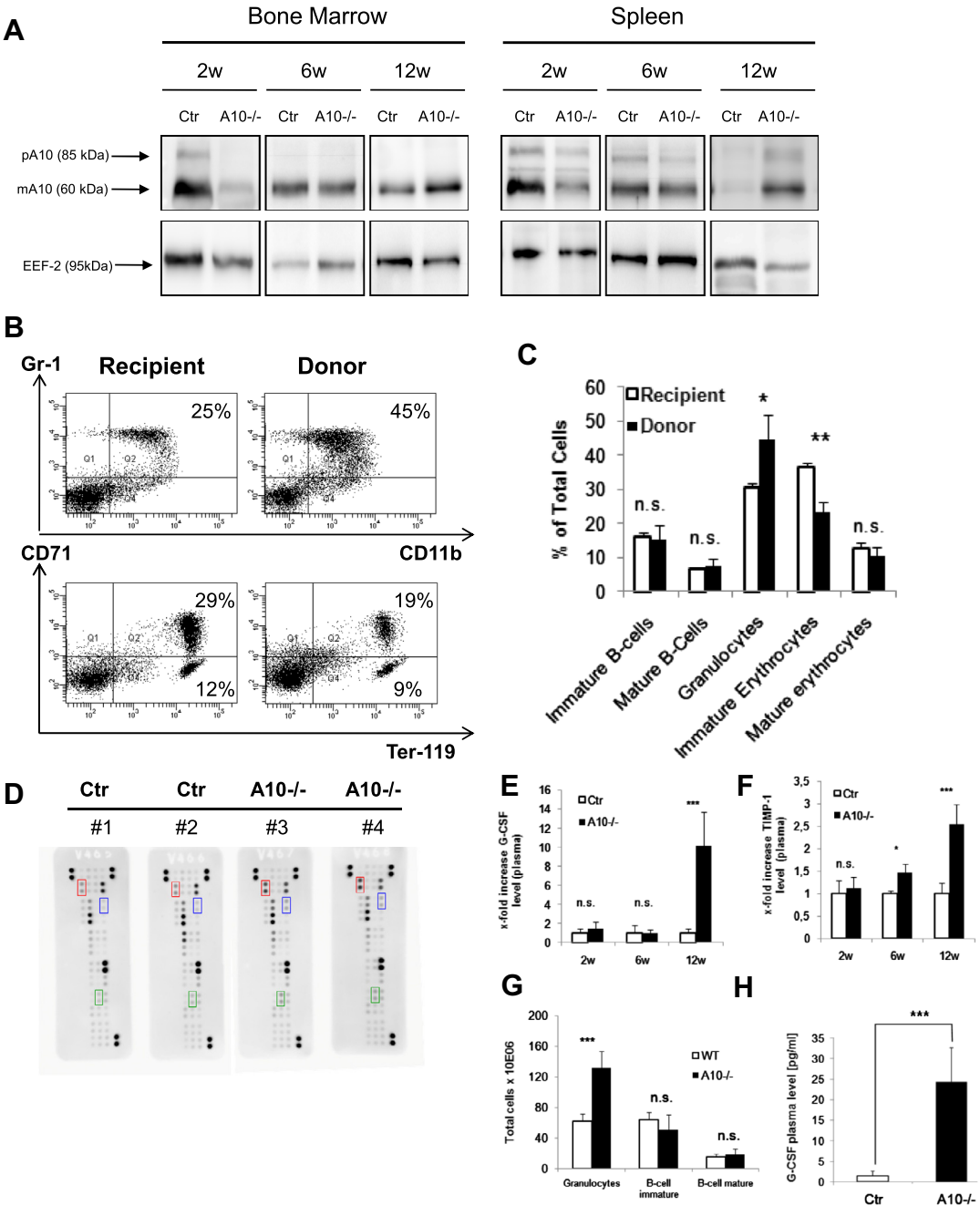

Fig. 4. Myeloproliferative disorder in ADAM10$^{-/-}$ mice is mediated by a non-cell autonomous mechanism and leads to an increase in plasma levels of G-CSF and TIMP-1. (A) Western Blot analysis of cell homogenates from bone marrow and spleen showing ADAM10 expression. pA10: precursor of ADAM10; mA10: mature form of ADAM10 (2, 6 and 12 weeks after pI–pC induction). EEF-2: Eukaryotic Elongation Factor-2 was used a loading control. (B) Bone marrow transplantation experiment: the percentage of myeloid (immunostaining with CD11b and Gr-1 specific antibodies) and erythroid cells (immunostaining with Ter-119 and CD71 specific antibodies) in the bone marrow of donor and recipient mice was determined by flow cytometry. (C) Flow cytometric analysis of different cell populations in the bone marrow of donor and recipient mice did not show changes in other cell populations than myeloid or erythroid cells. (D) Proteome Profiler array of 42 different cytokines revealed significant upregulation of G-CSF (red box), TIMP-1 (blue box) and IL-16 (green box) in ADAM10-deleted mice. ELISA measurements revealed strongly elevated levels of the cytokine G-CSF (E) and Tissue Inhibitor of Metalloprotease-1 (TIMP-1) (F). (G) Determination of total cell counts after 40 days of ADAM10 deletion in epidermis (K5-tTA-Cre ADAM10 mice). (H) ELISA measurement revealed strongly elevated levels of the cytokine G-CSF in plasma of K5-tTA-Cre ADAM10 cKO mice, 40 days after ADAM10 deletion $n > 4$ for each genotype. Error bars represent SEM. *P*-values: $^{*}P < 0.05$, $^{**}P < 0.005$, $^{***}P < 0.0005$. (For interpretation of the references to color in this figure legend, the reader is referred to the web version of this article.)

the LysM-Cre deleter strain (Supplementary Fig. 1). We could not detect any overt phenotypical changes in these mice as judged by flow cytometry, histological and biochemical analysis (data not shown) suggesting that ADAM10 is dispensable for terminal myeloid differentiation. The observed myeloproliferative disorder in the Mx-Cre cKO mice is not predominantly initiated by a cell-autonomous mechanism. Reevaluation of ADAM10 protein expression in hematopoietic cells from different tissues of ADAM10 knockout mice (Mx-Cre) after 2, 6 and 12 weeks following induction supported this hypothesis. As shown before, ADAM10 protein expression in bone marrow, spleen and liver (Fig. 1B) was significantly down regulated 2 weeks after the induction of the knockout with pI–pC. However, in induced ADAM10 knockout mice a re-expression of ADAM10 in bone marrow and spleen from 6 weeks onwards could be observed (Fig. 4A).

3.7. A non-cell autonomous mechanism for the development of the myeloproliferative disorder is mediated by bone marrow stroma cells

Bone marrow cells from pI–pC induced ADAM10-deficient mice (donor) were exchanged with bone marrow cells of pI–pC induced control mice (recipients). Flow cytometric analysis to determine granulocyte and erythrocyte distribution was performed in bone marrow of donor and recipient mice 6 weeks after the last pI–pC injection and subsequent BMT (Fig. 4B and C). These experiments demonstrated that transplantation of wildtype bone marrow to knockout mice still leads to MPD, but transplantation of knockout bone marrow to wildtype did not, strongly suggesting that ADAM10-deficiency in stroma cells causes the MPD.

3.8. Cytokine release in Mx-Cre driven and epidermis-specific ADAM10 knockouts triggers myeloproliferative disorders

We performed comprehensive cytokine analysis in plasma samples of ADAM10-deficient and control mice (Fig. 4D). Out of 42 different cytokines only 3 were significantly changed: TIMP-1, IL-16 and G-CSF. ELISA measurements (Fig. 4E and F) confirmed the increase of G-CSF and TIMP-1 in plasma over time. These results resemble the phenotype of conditional knockout mice with an induced epidermis-specific deletion of ADAM10 that was initially described by us before [12]. Also in these mice we observed an expansion of bone marrow cells with increased size and high granularity (data not shown), which were identified as granulocytes as judged by staining of the cells with antibodies against the myeloid markers CD11b and Gr-1 (Fig. 4G). Increased plasma level of G-CSF was another key observation during myeloid expansion after epidermis specific inactivation of ADAM10 (Fig. 4H) arguing for a similar process explaining the progression and sustainment of the MPD in these two (Mx-Cre and K5-tTA-Cre) transgenic mouse models.

4. Discussion and conclusion

Since the metalloproteinase ADAM10 is a well-known control point to modulate cell–cell contacts [13,14] we aimed to analyze if this protease plays a cell autonomous or a non-cell autonomous role in the hematopoiesis of adult mice. With the generation of conditional ADAM10-deficient mice under the control of the interferon-inducible Mx-promoter we were able to address this question. The different time points chosen for our analysis resemble the chronic and acceleration phases of MPD patients. Although successful excision of the floxed ADAM10 allele and subsequent downregulation of the ADAM10 protein within differentiated and a limited subset of hematopoietic progenitor cells after 2 weeks of pI–pC induction was observed, we detected a reappearance of cells with unexcised ADAM10 alleles already 6 weeks after induction. This observation suggests a competitive advantage for the hematopoietic progenitors in which excision did not occur. Interestingly, the severity of the described myeloproliferative disorder in ADAM10-deficient mice did not attenuate with the reemerging ADAM10 expression in hematopoietic cells, thereby suggesting primarily non-cell autonomous mechanisms involved in the progression of the MPD. The results of our BMT experiments confirmed this hypothesis.

The expression of ADAM10 in bone marrow stroma cells was revealed in various studies before [15–17]. The bone marrow transplantation experiments performed in this study suggest that the MPD phenotype is due to a lack of ADAM10 in non-hematopoetic cells. Alterations in bone marrow stromal cells are likely to be causative for the observed pathology and the role of ADAM10 in these cells deserves future investigations. According to previous mouse studies with (inducible) conditional ADAM10 inactivation [9,12,18,19], ADAM10 downregulation resembled Notch signaling-defective mutant mice [20–22]. Therefore it seems likely that ADAM10 is also a major upstream regulator of Notch signaling in bone marrow stroma cells *in vivo*.

Plasma analysis revealed a specific upregulation of G-CSF, TIMP-1 and IL-16. Interestingly TIMP-1 is known to be an endogenous inhibitor of ADAM10 activity [23] and might therefore act as a compensatory mechanism for upregulated ADAM10 activity due to increased numbers of granulocytes expressing high amounts of cell surface ADAM10. In Notch signaling-defective transgenic mice, a reduction of circulating G-CSF levels led to a rescue of many but not all of the observed phenotypes [9,24] strengthening our idea that TIMP-1 and IL-16 play an additional role for the development and the progression of the MPD.

The predominant role of G-CSF was supported by our observations in an inducible knockout of ADAM10 in the epidermis, which also displayed a myeloid expansion by a systemic, G-CSF-mediated mechanism. Therefore it seems likely that reducing ADAM10 activity in adult mice may lead to the formation of myeloproliferative disorders.

Since ADAM10 was proposed to be an attractive target for clinical therapy of various diseases like cancer [25,26], skin diseases [13,27,28] allergies or asthma [29–31] patients receiving ADAM10 modulating agents should be carefully monitored for a hematopoietic phenotype as observed in the conditional knockout mouse models described in this report.

Acknowledgments

This work was supported by the Deutsche Forschungsgemeinschaft SFB877. M.D. is supported by the Netherlands Heart Foundation (Dr. E. Dekker post-doctoral fellow Grant 2007T034 and 2012T079).

Appendix A. Supplementary data

Supplementary data associated with this article can be found, in the online version, at http://dx.doi.org/10.1016/j.bbrc.2013.11.020.

References

[1] K. Tanigaki, T. Honjo, Regulation of lymphocyte development by Notch signaling, Nat. Immunol. 8 (2007) 451–456.
[2] H. Han, K. Tanigaki, N. Yamamoto, K. Kuroda, M. Yoshimoto, T. Nakahata, K. Ikuta, T. Honjo, Inducible gene knockout of transcription factor recombination signal binding protein-J reveals its essential role in T versus B lineage decision, Int. Immunol. 14 (2002) 637–645.
[3] K. Reiss, A. Ludwig, P. Saftig, Breaking up the tie: disintegrin-like metalloproteinases as regulators of cell migration in inflammation and invasion, Pharmacol. Ther. 111 (2006) 985–1006.

[4] R.M. Wang, Y.G. Song, Y.F. Han, Effect of rare earth on the microstructures and properties of a low expansion superalloy, Micron 33 (2002) 575–580.
[5] D. Hartmann, B. de Strooper, L. Serneels, K. Craessaerts, A. Herreman, W. Annaert, L. Umans, T. Lubke, A. Lena Illert, K. von Figura, P. Saftig, The disintegrin/metalloprotease ADAM 10 is essential for Notch signalling but not for alpha-secretase activity in fibroblasts, Hum. Mol. Genet. 11 (2002) 2615–2624.
[6] P. Sinha, O. Chornoguz, V.K. Clements, K.A. Artemenko, R.A. Zubarev, S. Ostrand-Rosenberg, Myeloid-derived suppressor cells express the death receptor Fas and apoptose in response to T cell-expressed FasL, Blood 117 (2011) 5381–5390.
[7] B.E. Clausen, C. Burkhardt, W. Reith, R. Renkawitz, I. Forster, Conditional gene targeting in macrophages and granulocytes using LysMcre mice, Transgenic Res. 8 (1999) 265–277.
[8] M.K. Srivastava, P. Sinha, V.K. Clements, P. Rodriguez, S. Ostrand-Rosenberg, Myeloid-derived suppressor cells inhibit T-cell activation by depleting cystine and cysteine, Cancer Res. 70 (2010) 68–77.
[9] M. Yoda, T. Kimura, T. Tohmonda, S. Uchikawa, T. Koba, J. Takito, H. Morioka, M. Matsumoto, D.C. Link, K. Chiba, Y. Okada, Y. Toyama, K. Horiuchi, Dual functions of cell-autonomous and non-cell-autonomous ADAM10 activity in granulopoiesis, Blood 118 (2011) 6939–6942.
[10] R. Kuhn, F. Schwenk, M. Aguet, K. Rajewsky, Inducible gene targeting in mice, Science 269 (1995) 1427–1429.
[11] I. Diamond, T. Owolabi, M. Marco, C. Lam, A. Glick, Conditional gene expression in the epidermis of transgenic mice using the tetracycline-regulated transactivators tTA and rTA linked to the keratin 5 promoter, J. Invest. Dermatol. 115 (2000) 788–794.
[12] S. Weber, M.T. Niessen, J. Prox, R. Lullmann-Rauch, A. Schmitz, R. Schwanbeck, C.P. Blobel, E. Jorissen, B. de Strooper, C.M. Niessen, P. Saftig, The disintegrin/metalloproteinase Adam10 is essential for epidermal integrity and Notch-mediated signaling, Development 138 (2011) 495–505.
[13] G. Chaimowitz, Psychotherapy training of psychiatrists, Can. J. Psychiatry 56 (2011) 1.
[14] B. Schulz, J. Pruessmeyer, T. Maretzky, A. Ludwig, C.P. Blobel, P. Saftig, K. Reiss, ADAM10 regulates endothelial permeability and T-Cell transmigration by proteolysis of vascular endothelial cadherin, Circ. Res. 102 (2008) 1192–1201.
[15] A. Hikita, I. Yana, H. Wakeyama, M. Nakamura, Y. Kadono, Y. Oshima, K. Nakamura, M. Seiki, S. Tanaka, Negative regulation of osteoclastogenesis by ectodomain shedding of receptor activator of NF-kappaB ligand, J. Biol. Chem. 281 (2006) 36846–36855.
[16] C. Bret, D. Hose, T. Reme, A. Kassambara, A. Seckinger, T. Meissner, J.F. Schved, T. Kanouni, H. Goldschmidt, B. Klein, Gene expression profile of ADAMs and ADAMTSs metalloproteinases in normal and malignant plasma cells and in the bone marrow environment, Exp. Hematol. 39 (2011) 546–557. e548.
[17] M.R. Zocchi, S. Catellani, P. Canevali, S. Tavella, A. Garuti, B. Villaggio, A. Zunino, M. Gobbi, G. Fraternali-Orcioni, A. Kunkl, J.L. Ravetti, S. Boero, A. Musso, A. Poggi, High ERp5/ADAM10 expression in lymph node microenvironment and impaired NKG2D-ligands recognition in Hodgkin lymphomas, Blood 119 (2012) 1479–1489.
[18] E. Jorissen, J. Prox, C. Bernreuther, S. Weber, R. Schwanbeck, L. Serneels, A. Snellinx, K. Craessaerts, A. Thathiah, I. Tesseur, U. Bartsch, G. Weskamp, C.P. Blobel, M. Glatzel, B. De Strooper, P. Saftig, The disintegrin/metalloproteinase ADAM10 is essential for the establishment of the brain cortex, J. Neurosci. 30 (2010) 4833–4844.
[19] D.R. Gibb, M. El Shikh, D.J. Kang, W.J. Rowe, R. El Sayed, J. Cichy, H. Yagita, J.G. Tew, P.J. Dempsey, H.C. Crawford, D.H. Conrad, ADAM10 is essential for Notch2-dependent marginal zone B cell development and CD23 cleavage in vivo, J. Exp. Med. 207 (2010) 623–635.
[20] Y. Qyang, S.M. Chambers, P. Wang, X. Xia, X. Chen, M.A. Goodell, H. Zheng, Myeloproliferative disease in mice with reduced presenilin gene dosage: effect of gamma-secretase blockage, Biochemistry 43 (2004) 5352–5359.
[21] L. Zhou, L.W. Li, Q. Yan, B. Petryniak, Y. Man, C. Su, J. Shim, S. Chervin, J.B. Lowe, Notch-dependent control of myelopoiesis is regulated by fucosylation, Blood 112 (2008) 308–319.
[22] Y.W. Kim, B.K. Koo, H.W. Jeong, M.J. Yoon, R. Song, J. Shin, D.C. Jeong, S.H. Kim, Y.Y. Kong, Defective Notch activation in microenvironment leads to myeloproliferative disease, Blood 112 (2008) 4628–4638.
[23] A. Amour, C.G. Knight, A. Webster, P.M. Slocombe, P.E. Stephens, V. Knauper, A.J. Docherty, G. Murphy, The in vitro activity of ADAM-10 is inhibited by TIMP-1 and TIMP-3, FEBS Lett. 473 (2000) 275–279.
[24] A. Dumortier, A.D. Durham, M. Di Piazza, S. Vauclair, U. Koch, G. Ferrand, I. Ferrero, S. Demehri, L.L. Song, A.G. Farr, W.J. Leonard, R. Kopan, L. Miele, D. Hohl, D. Finke, F. Radtke, Atopic dermatitis-like disease and associated lethal myeloproliferative disorder arise from loss of Notch signaling in the murine skin, PLoS One 5 (2010) e9258.
[25] P.C. Liu, X. Liu, Y. Li, M. Covington, R. Wynn, R. Huber, M. Hillman, G. Yang, D. Ellis, C. Marando, K. Katiyar, J. Bradley, K. Abremski, M. Stow, M. Rupar, J. Zhuo, Y.L. Li, Q. Lin, D. Burns, M. Xu, C. Zhang, D.Q. Qian, C. He, V. Sharief, L. Weng, C. Agrios, E. Shi, B. Metcalf, R. Newton, S. Friedman, W. Yao, P. Scherle, G. Hollis, T.C. Burn, Identification of ADAM10 as a major source of HER2 ectodomain sheddase activity in HER2 overexpressing breast cancer cells, Cancer Biol. Ther. 5 (2006) 657–664.
[26] D.R. Gibb, S.J. Saleem, D.J. Kang, M.A. Subler, D.H. Conrad, ADAM10 overexpression shifts lympho- and myelopoiesis by dysregulating site 2/site 3 cleavage products of Notch, J. Immunol. 186 (2011) 4244–4252.
[27] T. Maretzky, F. Scholz, B. Koten, E. Proksch, P. Saftig, K. Reiss, ADAM10-mediated E-cadherin release is regulated by proinflammatory cytokines and modulates keratinocyte cohesion in eczematous dermatitis, J. Invest. Dermatol. 128 (2008) 1737–1746.
[28] I. Inoshima, N. Inoshima, G.A. Wilke, M.E. Powers, K.M. Frank, Y. Wang, J. Bubeck Wardenburg, A *Staphylococcus aureus* pore-forming toxin subverts the activity of ADAM10 to cause lethal infection in mice, Nat. Med. 17 (2011) 1310–1314.
[29] M. von Planta, M.H. Weil, R.J. Gazmuri, M.A. Ritz, E.C. Rackow, Calcium-entry blockers during porcine cardiopulmonary resuscitation, Clin. Sci. (Lond.) 78 (1990) 207–213.
[30] N.S. Chaimowitz, R.K. Martin, J. Cichy, D.R. Gibb, P. Patil, D.J. Kang, J. Farnsworth, E.C. Butcher, B. McCright, D.H. Conrad, A disintegrin and metalloproteinase 10 regulates antibody production and maintenance of lymphoid architecture, J. Immunol. 187 (2011) 5114–5122.
[31] N.S. Chaimowitz, R.K. Martin, J. Cichy, D.R. Gibb, P. Patil, D.J. Kang, J. Farnsworth, E.C. Butcher, B. McCright, D.H. Conrad, A disintegrin and metalloproteinase 10 regulates antibody production and maintenance of lymphoid architecture, J. Immunol. 187 (2011) 5114–5122.